Cardiology Journal

VIA MEDICA

ORIGINAL ARTICLE

DOI: 10.5603/cj.90744

ISSN 1897–5593
eISSN 1898–018X

Diagnostic accuracy of a novel optical coherence tomography-based fractional flow reserve algorithm for assessment of coronary stenosis significance

Weili Pan[1]*, Wenjuan Wei[2]*, Yumeng Hu[3]*, Li Feng[3], Yongkui Ren[1], Xinsheng Li[1], Changling Li[4], Jun Jiang[4], Jianping Xiang[3], Xiaochang Leng[3], Da Yin[1, 5]

[1]Department of Cardiology, The First Affiliated Hospital of Dalian Medical University, Dalian, China
[2]Department of Cardiology, The First People's Hospital of Xiaoshan District, Hangzhou, China
[3]ArteryFlow Technology Co., Ltd., Hangzhou, China
[4]Department of Cardiology, The Second Affiliated Hospital, Zhejiang University School of Medicine, Hangzhou, China
[5]Department of Cardiology, Shenzhen Cardiovascular Minimally Invasive Medical Engineering Technology Research and Development Center, Shenzhen People's Hospital, Shenzhen, China

Abstract

Background: *This study aimed to propose a novel computational approach for assessing physiological significance of coronary lesions from optical coherence tomography (OCT), and to evaluate its diagnostic performance.*

Methods: *A novel fractional flow reserve (FFR) algorithm (AccuFFRoct) based on the fusion of OCT and coronary angiography was developed to evaluate functional ischemia of coronary stenosis. Thirty-four consecutive patients underwent coronary angiography, OCT and FFR were included, and AccuFFRoct was used to calculate the FFR for all patients. The diagnostic performance of AccuFFRoct was compared with the wire-measured FFR reference standard.*

Results: *Per vessel accuracy, sensitivity, specificity, positive predictive value and negative predictive value for AccuFFRoct in identifying hemodynamically significant coronary stenosis were 93.8%, 94.7%, 92.3%, 94.7%, and 92.3%, respectively. Good correlation (correlation coefficient $r = 0.80$, $p < 0.001$) between AccuFFRoct and FFR was observed. The Bland-Altman analysis showed a mean difference of –0.037 (limits of agreement: –0.189 to 0.115). The area under the curve (AUC) of AccuFFRoct in identifying physiologically significant stenosis was 0.94, which was higher than that of minimum lumen area (AUC = 0.91) and significantly higher than diameter stenosis (AUC = 0.78).*

Conclusions: *The study demonstrated high efficiency and accuracy of AccuFFRoct for clinical implementation in functional assessment of coronary artery disease. It could provide additional insights beyond current coronary imaging-based anatomical assessment, aiding in clinical decision-making.* (Cardiol J)

Keywords: optical coherence tomography, coronary angiography, fractional flow reserve

Address for correspondence: Da Yin, MD, Department of Cardiology, Shenzhen Cardiovascular Minimally Invasive Medical Engineering Technology Research and Development Center, Shenzhen People's Hospital, 1017 Dongmen North Road, Shenzhen 518020, China, tel: +86 0755 2553 3018, e-mail: szyinda@hotmail.com; Xiaochang Leng, PhD, ArteryFlow Technology Co., Ltd., 459 Qianmo Road, Hangzhou 310051, China, tel: +86 0571 8677 2567, e-mail: xiaochang.leng@arteryflow.com; Jianping Xiang, PhD, ArteryFlow Technology Co., Ltd., 459 Qianmo Road, Hangzhou 310051, China, tel: +86 0571 8677 2567, e-mail: jianping.xiang@arteryflow.com

Received: 28.06.2022 Accepted: 15.10.2023 Early publication date: 9.11.2023

**These authors contributed equally to this work.*

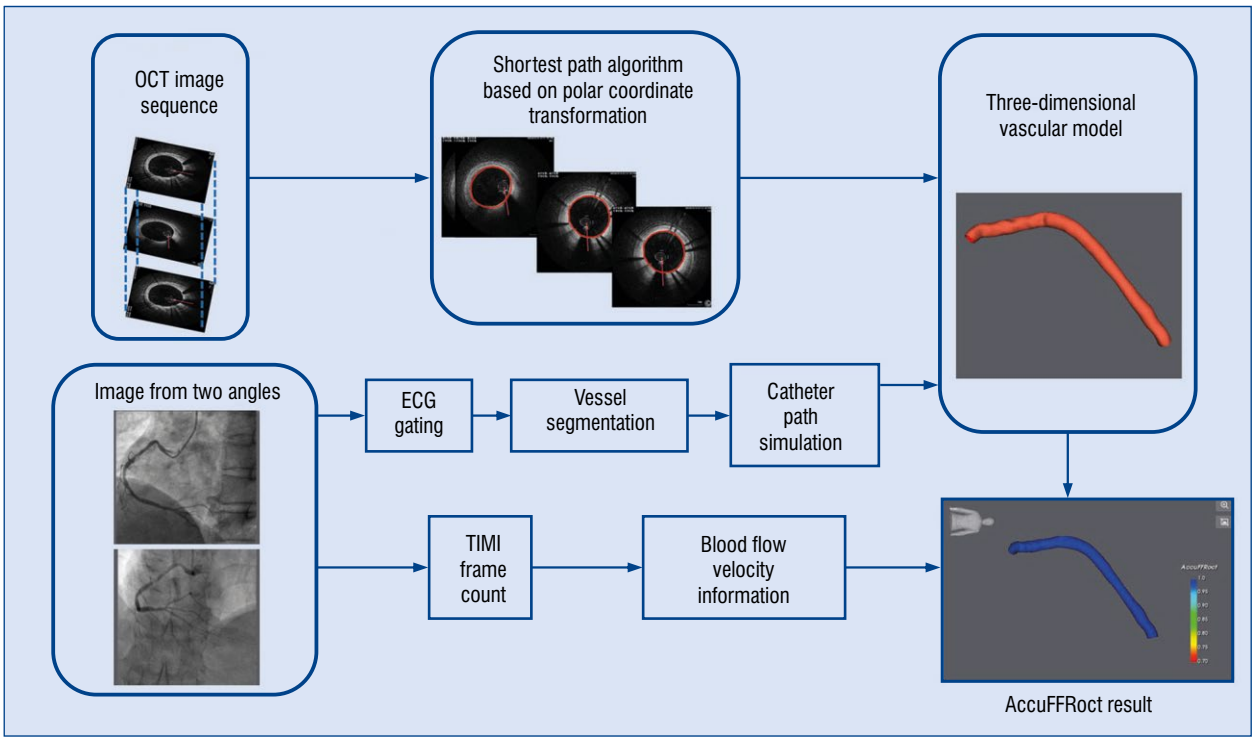

Figure 1. Workflow for coronary artery reconstruction from coronary angiography and optical coherence tomography (OCT) images; ECG — electrocardiogram; TIMI — thrombolysis in myocardial infarction.

Introduction

Coronary artery disease (CAD) is the leading cause of mortality worldwide [1]. Different revascularization strategies have been explored to improve the prognosis of patients with CAD. Accumulating evidence has demonstrated that plaque morphology and functional assessment of coronary lesions are the two main cornerstones of clinical decision-making [2, 3]. Clinically, optical coherence tomography (OCT) is an intracoronary imaging modality with the highest resolution, and it can precisely identify vessel lumen and plaque characteristics [2]. Meanwhile, invasive pressure wire-based fractional flow reserve (FFR) is the gold standard for assessing coronary physiological function [3]. OCT and FFR can help optimize percutaneous coronary intervention (PCI) of coronary lesions from morphological and functional aspects.

Previous studies have demonstrated that OCT- and FFR-guided PCI can lead to favorable outcomes compared with angiography-guided PCI [3, 4]. However, combined utilization of the two imaging modalities is restricted, partly due to the costs and procedural complexity involved. Fortunately, several OCT-derived computational methods for FFR estimation have been developed, which are consistent with wire-based FFR measurements to a certain extent and have showed superiority to angiography-based computational FFR [5–7]. Although the initial results are promising, these methods still need improvement to increase clinical feasibility. In the present study, we developed a novel and fast algorithm to compute OCT-derived FFR and evaluated its diagnostic performance for detecting lesion-specific ischemia.

Methods

This study introduced a robust approach for three-dimensional (3D) reconstruction of coronary arteries by combining angiographic images, OCT images, and fast computation of FFR. Computation of AccuFFRoct was performed using a prototype software (AccuFFRoct, ArteryFlow Technology, Hangzhou, China). The overall workflow of the AccuFFRoct calculation is shown in Figure 1. Comparison with invasive FFR was made to validate the feasibility and diagnostic performance of this approach.

Study population

To evaluate the above-mentioned OCT-derived FFR approach, 34 consecutive patients who had un-

dergone coronary angiography (CAG), OCT, and FFR measurement were recruited in this study. The C7--XR/ILUMIEN OPTIS OCT intravascular imaging system (St. Jude Medical, St. Paul, MN, USA) was used to acquire OCT images, and a QUANTIEN TM measurement system (St. Jude. Medical, St. Paul, MN, USA) was applied to measure FFR. Exclusion criteria were as follows: 1) OCT images with vessel spasm or injury during imaging; 2) OCT pullback was too short to cover the whole lesion; 3) The quality of angiographic images were so poor that the vessel boundary could not be distinguished; and 4) angiographic images without two appropriate angles or with severe overlapping.

Angiographic image processing

Geometry parameter calibration

First, two coronary angiography sequences with angle differences at least 25° should be selected. These two images must be of high quality and contain the same vessel that needs to be reconstructed.

Because the cardiac motion at the end-diastole is minimal in the cardiac cycle, this phase is preferred for optimal reconstruction in the system. Electrocardiogram (ECG) gating is applied to determine the appropriate cardiac phase selection if an ECG signal is available. Calibration of image acquisition parameters is essential to eliminate geometrical errors and achieve optimal correspondence between the two images. In the angiography system, three pairs of physiological points are required to represent corresponding landmark points on the vessel. Typically, priority is given to selecting the bifurcation and lesion as landmark points.

Segmentation of coronary angiography

The precise centerline of the target vessel is a prerequisite for segmentation of angiographic images. After determine the centerline, the original image is preprocessed by resampling along scanlines that are perpendicular to the centerline. A cost image is generated for further segmentation using the reciprocal of the weighted sum of the first and second derivative of the brightness distribution along the scanline.

Among all the resampling points in the cost image, points on the lumen borders tend to have lower cost values. Therefore, we define the starting point and the endpoint with the lowest cost value, located in the first scanline and last scanline, respectively. The Dijkstra minimum path algorithm is ultimately used to determine the vessel lumen boundaries [8, 9].

3D lumen outline

Based on the finite projective camera model and existing optimization methods, an algorithm for the 3D reconstruction of coronary arteries from two views of uncalibrated angiographic images is proposed [10]. After calibrating of the image acquisition parameters, each point on the centerline in 3D space corresponds to a 2D coordinate at two different projection planes in different points of view. This slice of the geometry is composed of four key boundary points in the cross-section centered at the point of the centerline. Scanning from the proximal points to the distal points finally reconstructs the entire vessel lumen.

Estimation of catheter

The trajectory of the OCT catheter in the vessel is derived using a graph theory algorithm [11]. Firstly, the total energy (the sum of internal and elastic energy) is calculated at each cross-section of the vessel geometry segmented from coronary angiography. Based on this, the catheter trajectory is determined according to the principle of minimum energy [10].

OCT image processing

Automatic OCT segmentation

The first frame was extracted and resampled based on bilinear interpolation with the origin at the center of the image. The starting point was chosen as the pixel with the highest intensity. The initial segmentation of the lumen border was derived with Dijkstra's shortest-path algorithm.

The boundary of the lumen was refined by again using the Dijkstra's shortest-path algorithm, by defining contour points as the source and resampling the image using bilinear interpolation along the normal direction. Once the segmentation contour was obtained on the first frame, the boundary was mapped onto the next frame. The final segmentation results of the entire OCT sequences can be obtained by repeating the image processing above.

Coronary artery modeling

Fusion of OCT and X-ray angiographic images

It should be noted that the OCT catheter twists and bends within the vascular vessel. Therefore, to ensure the morphological characteristics of the vessel are preserved, the OCT borders are stacked in the correct orientation along the calculated guide wire trajectory.

AccuFFRoct calculation

Average flow rate from frame count

In this section, we introduce the thrombolysis in myocardial infarction (TIMI) frame count as

a method to derive patient-specific blood flow information for precise FFR. This involves counting the number of frames during which period the blood flows from the proximal to the distal segment [12], which allows for estimation of the blood flow rate in the target vessel. Then, the blood flow velocity for FFR calculation can be determined based on the flow rate and the arterial geometrical characteristics. It should be noted that angiographic images are typically collected at rest, while wired-based FFR is measured under the condition of maximal hyperemia. Thus, a flow rate conversion relationship is applied to estimate the flow at hyperemia [13].

FFR calculation

The next step is to quantify the degree of stenosis by extracting geometrical characteristics and estimating the reference vessel diameter. Using this information, the pressure drop of blood flowing across the lesions can be calculated [10]. The mean aortic pressure at rest was obtained from the monitor and multiplied by a factor to estimate the hyperemic aortic pressure [14]. AccuFFRoct values were then calculated as the ratio of the mean distal coronary pressure and the mean proximal aortic pressure, in accordance with the definition.

Ethics approval

The study was conducted in accordance with the Declaration of Helsinki and Good Clinical Practice. The study was approved by the Ethics Committee of The First Affiliated Hospital of Dalian Medical University, and individual consent for this retrospective analysis was waived according to Measures for the Ethical Review of Biomedical Research Involving Humans published by the National Health Commission of China (CLI.4.282697).

Statistical analysis

Continuous variables were presented as mean ± standard deviation (SD), binary variables were presented as percentages. The correlation between AccuFFRoct and invasive wire-measured FFR was evaluated by Pearson's or Spearman's correlation analysis. The Bland-Altman analysis was implemented to characterize the agreement between AccuFFRoct and invasive FFR. The diagnostic performance of AccuFFRoct (≤ 0.8) was evaluated by the area under the receiver-operating characteristic curve (AUC). Anatomic characteristics such as minimal lumen area (MLA), diameter stenosis (DS%) were also analyzed using FFR ≤ 0.8 as the reference standard. The statistical significance was represented by a 2-sided p-value (< 0.05). All statistical analyses were performed using MedCalc (version 19.0, MedCalc Software, Ostend, Belgium).

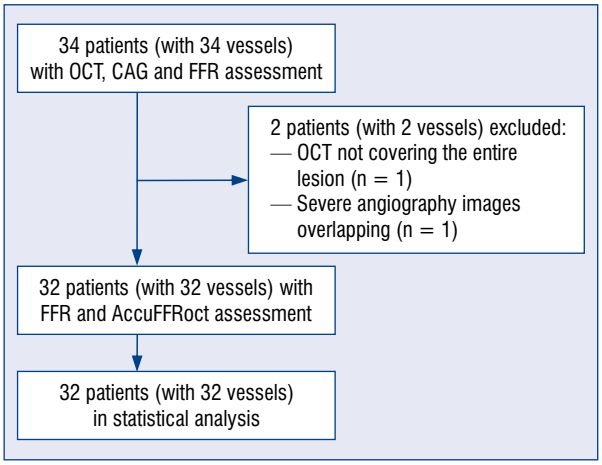

Figure 2. Participant flow chart of the study; CAG — coronary angiography; FFR — fractional flow reserve; OCT — optical coherence tomography.

Results

Baseline clinical and lesion characteristics

A total of 34 consecutive patients who underwent, coronary angiography, OCT, and invasive FFR were enrolled in this study. Two patients were excluded: one due to the OCT not covering the entire lesion and one due to severe image overlap. Thus, AccuFFRoct analysis was performed in 32 vessels in 32 patients; the participant flow chart of the study is shown in Figure 2. Among all interrogated lesions, 13 (40.6%) were in the left anterior descending artery (LAD), 11 (34.4%) were in the left circumflex artery (LCX), and 8 (25.0%) were in the right coronary artery (RCA). The mean invasive FFR value was 0.77 ± 0.13; more than half (59.4%) of the lesions had FFR ≤ 0.80. Detailed clinical and lesion characteristics are presented in Table 1.

Agreement between AccuFFRoct and FFR

An example of AccuFFRoct calculation of the RCA artery is shown in Figure 3. The calculated AccuFFRoct value was 0.97, which matched well with the FFR (0.95) measured by pressure wire. AccuFFRoct had an average value of 0.80 ± 0.11. As shown in Figure 4, a good correlation (Pearson's correlation coefficient: $r = 0.80$, $p < 0.001$) between FFR and AccuFFRoct was observed. The Bland-Altman analysis is presented in Figure 5, which showed a mean difference value of –0.037

Table 1. Baseline characteristics.

Clinical characteristics	N = 32
Age [year]	56 ± 10
Male	68.8% (22)
Weight [kg]	63.8 ± 11
Height [cm]	170.8 ± 7.5
BMI [kg/m^2]	25.2 ± 2.6
Systolic blood pressure [mmHg]	141.3 ± 21
Diastolic blood pressure [mmHg]	81.3 ± 11.7
Heart rate [beats/min]	70.8 ± 11.3
Breath [breaths/min]	17.8 ± 0.7
Hypertension	37.5% (12)
Hypercholesterolemia	25.0% (8)
Diabetes mellitus	15.6% (5)
Smoking history	37.5% (12)
Old myocardial infraction	9.4% (3)
Previous PCI	12.5% (4)
Vessels:	
LAD	40.6% (13)
LCX	34.4% (11)
RCA	25.0% (8)
Bifurcation lesions	37.5% (12)
Tandem lesions	25.0% (8)
Anatomy:	
Diameter stenosis	48.5 ± 10.3%
< 50%	53.1% (17)
≥ 50%	46.9% (15)
MLA [mm^2]	
≤ 1.71	50.0% (16)
> 1.71	50.0% (16)
Physiology:	
FFR	0.77 ± 0.13
Vessels with FFR ≤ 0.8	59.4% (19)
Vessels with FFR > 0.8	40.6% (13)

BMI — body mass index; FFR — fractional flow reserve; LAD — left anterior descending artery; LCX — left circumflex artery; MLA — minimum lumen area; PCI — percutaneous coronary intervention; RCA — right coronary artery

(limits of agreement: –0.189 to 0.115). The mean difference between FFR and AccuFFRoct was –0.037 ± ± 0.08, indicating a good agreement, but a very slight underestimation of AccuFFRoct was observed.

Diagnostic performance of AccuFFRoct, OCT, and CAG

The diagnostic accuracy of AccuFFRoct in detecting FFR ≤ 0.8 was 93.8% (95% CI 79.2–99.2), with 18 true positives, 12 true negatives, one false positive, and one false negative, corresponding to the sensitivity, specificity, positive predictive value (PPV), negative predictive value (NPV), positive likelihood ratio (+LR), and negative likelihood ratio (–LR) of 94.7%, 92.3%, 94.7%, 92.3%, 12.3, and 0.06, respectively (Table 2).

The AUC of AccuFFRoct in identifying physiologically significant stenosis was 0.94 (95% CI 0.80–0.99), which was higher than MLA (AUC = = 0.91 [95% CI 0.76–0.98]) and significantly higher than DS% from CAG images (AUC = 0.78 [95% CI 0.60–0.91]), as presented in Figure 6. The best cutoff value for MLA was identified as ≤ 1.71 mm^2. The median processing time required for the computation of AccuFFRoct from the moment OCT data were loaded into the software was 4.90 (interquartile range: 2.59–7.21) minutes on a standard desktop workstation with 4.2 GHz Intel i7 8-core processor.

Repeated AccuFFRoct analysis was also performed. Intra- and inter-observer variability in AccuFFRoct analysis was 0.01 ± 0.03 and 0.01 ± 0.05, respectively.

Discussion

The salient findings of this study are the following: 1) A new approach (AccuFFRoct) for fast computation of FFR from OCT images was developed; 2) AccuFFRoct showed a strong correlation and good agreement with FFR in consecutive patients; 3) Using the cutoff value of FFR ≤ 0.80 for identifying the hemodynamic significance of coronary stenosis, AccuFFRoct showed an overall accuracy of 93.8%, sensitivity of 94.7%, and specificity of 92.3%; and 4) AccuFFRoct showed evident superior diagnostic performance to OCT-derived MLA and CAG-based DS%.

Significance of OCT-derived FFR

Pressure-derived FFR is the reference standard used to assess which coronary stenosis limits maximal blood flow, and to guide optimal therapy. A solid body of evidence and guideline recommendations have show that FFR-guided PCI brings CAD patients a better prognosis compared to CAG-guided PCI [3, 15, 16]. However, the clinical adoption of FFR remains disappointing in the real world due to the use of costly pressure wires, hyperemic agents, and complex procedures [17, 18]. To simplify the acquisition processes and increase the clinical application of FFR, several computational imaging-based methods for FFR estimation have been developed [5–7].

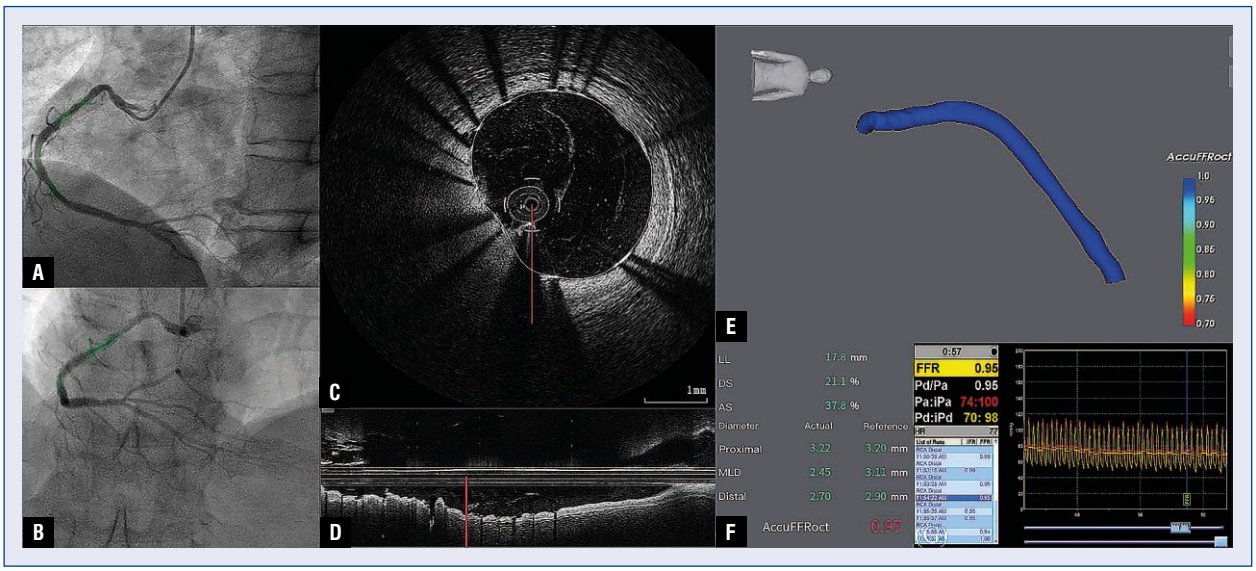

Figure 3. Example of AccuFFRoct calculation of the right coronary artery; **A, B.** Two images of coronary angiography showing the coronary stenosis; **C, D.** The images of the optical coherence tomography cross-section view and longitudinal view; **E.** AccuFFRoct calculation result distribution; **F.** The AccuFFRoct value was 0.97; **G.** The fractional flow reserve (FFR) measured by pressure wire was 0.95; LL — lesion length; DS — diameter stenosis; AS — area stenosis; MLD — minimum lumen diameter.

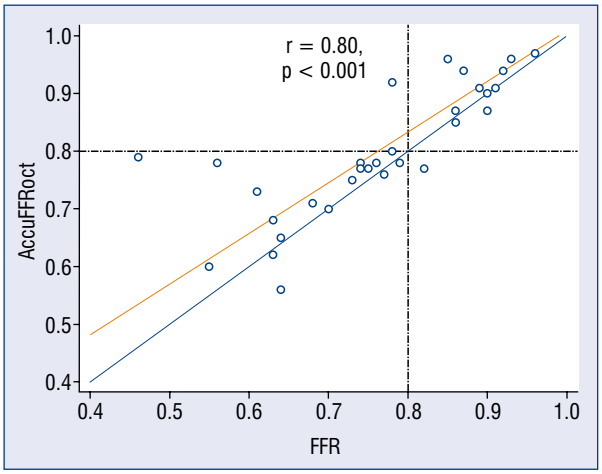

Figure 4. Correlation between wire-measured fractional flow reserve (FFR) and optical coherence tomography-derived FFR.

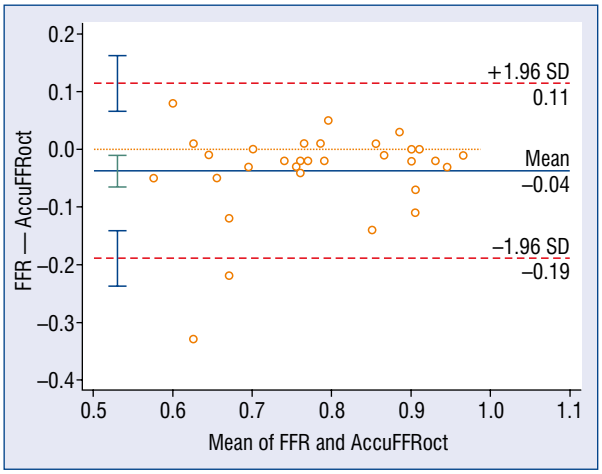

Figure 5. The Bland-Altman plots between optical coherence tomography-derived fractional flow reserve (FFR) (AccuFFRoct) and clinically measured FFR for the same vessels.

With the best resolution in all the imaging techniques, OCT provides a more accurate visualization of the arterial lumen, plaque, and vascular wall structures. Meanwhile, precise reconstruction of vessel dimensions is pivotal for the accurate computation of FFR. Therefore, the diagnostic performance of OCT-derived FFR is superior to CAG-based FFR [5]. In addition, OCT can guide the tailoring of treatment based on plaque morphology and identify stent malapposition and tissue prolapse to optimize stent implantation [2, 4]. In a recent prospective real-world analysis of 60 patients with intermediate stenoses, OCT-derived FFR demonstrated good diagnostic performance compared to FFR in predicting functional relevance with accuracy, sensitivity and specificity of 93%, 92%, and 93%, respectively [19]. By integrating the advantages offered by OCT in morphological

Table 2. Diagnostic performance of AccuFFRoct.

	AccuFFRoct ≤ 0.8 (95% CI)	DS% ≥ 50% (95% CI)	MLA ≤ 1.71 mm² (95% CI)
Accuracy [%]	93.75 (79.19–99.23)	68.75 (49.99–83.88)	84.38 (67.21–94.72)
Sensitivity [%]	94.74 (73.97–99.87)	63.16 (38.36–83.71)	78.95 (54.43–93.95)
Specificity [%]	92.31 (63.97–99.81)	76.92 (46.19–94.96)	92.31 (63.97–99.81)
Positive likelihood ratio	12.32 (1.87–81.20)	2.74 (0.96–7.82)	10.26 (1.54–68.44)
Negative likelihood ratio	0.06 (0.01–0.39)	0.48 (0.25–0.93)	0.23 (0.09–0.55)
Disease prevalence [%]	59.38 (40.64–76.30)	59.38 (40.64–76.30)	59.38 (40.64–76.30)
Positive predictive value [%]	94.74 (73.19–99.16)	80.00 (58.32–91.96)	93.75 (69.23–99.01)
Negative predictive value [%]	92.31 (63.89–98.79)	58.82 (42.48–73.43)	75.00 (55.33–87.90)

CI — confidence interval; DS% — percentage diameter stenosis; MLA — minimum lumen are

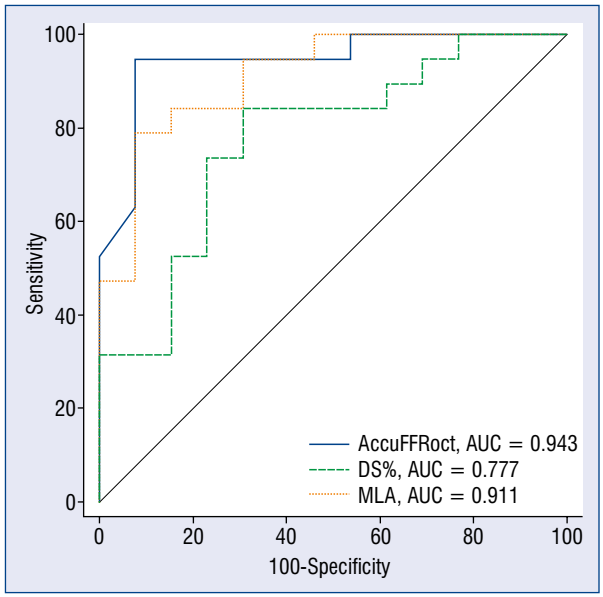

Figure 6. The area under curve (AUC) plots between optical coherence tomography-derived fractional flow reserve (FFR) (AccuFFRoct) and clinically measured FFR for the same vessels; DS% — percentage diameter stenosis; MLD — minimum lumen area.

assessment, including calcium detection, dissection identification and PCI optimization, with functional assessment through OCT-derived FFR, a one-stop-shop for obtaining all the information that needed for decision-making and achieving optimum outcomes for patients can be established [20]. This one-stop-shop approach provides a more holistic evaluation of the patient's condition.

In summary, the integration of coronary OCT imaging and physiological assessment is beneficial for a comprehensive evaluation of coronary lesions, enabling accurate diagnosis and tailored the treatment strategies, and significantly improving the prognosis of patients with CAD.

Advantages of AccuFFRoct

To date, several OCT-based FFR algorithms have been published, but the present method improved upon two pivotal points. Firstly, we took the curvature of blood vessels into account. Previous OCT reconstruction methods did not combine imaging registration, and the reconstruction images depict straight blood vessels, which are inconsistent with the normal anatomic structures of coronary arteries. In contrast, AccuFFRoct combines angiographic and OCT images to produce a more realistic 3D model of the vessel with curvature. Moreover, the differences in hemodynamics between curved and straight blood vessels may impair the accuracy of OCT-FFR. Secondly, we apply a TIMI frame count to calculate patient-specific flow velocities as inlet boundary condition. Previous methods assumed a fixed inlet velocity of 0.35 m/s (at hyperemia) [5–7], or resting flow of 10 cm/s (systolic) and 15 cm/s (end-diastolic), ignoring the individual differences. By using TIMI frame counting to calculate patient-specific flow velocities as inlet boundary conditions, the FFR results are more realistic and accurate. In addition, the entire calculation process takes approximately 5 min, which is more conducive to clinical application.

Limitations of the study

The study has several limitations. First, the validation of the present method was limited to a single-center with a small sample size, a larger multicenter studies are needed to further validate the diagnostic performance of the current method. Second, the reconstruction and evaluation of vessel segments with very distant stenosis is not possible

due to the limited length of the OCT catheter. Thus, for patients with global artery effects or long tandem lesions, the functional significance may not be fully assessed with this method. Third, combining OCT with CAG to some extent increased the complexity of this method, while this method didn't show significant superiority in diagnostic accuracy compared with other approaches, which may affect its clinical applicability. However, the advantage of OCT-FFR may be more pronounced in complex or borderline lesions, further studies are needed to verify the clinical value and potential advantage of this method. Finally, the study did not assess coronary microcirculation function. Therefore, the effects of coronary microcirculation dysfunction on the discordance between FFR and OCT-derived FFR were uncertain and require further investigation.

Conclusions

AccuFFRoct showed a strong correlation and good agreement with FFR, highlighting its potential as an efficient, accurate, and user-friendly tool in the catheterization laboratory. Its fast computation time and excellent semi-automatic workflow could provide valuable insights into coronary imaging and physiology for patients and clinical staff.

Funding

This work was supported by Zhejiang Provincial Public Welfare Technology Research Project (No. LGF20H020012), National Natural Science Foundation of China (No. 82170332), Zhejiang Provincial Key Research and Development Plan (No. 2020C03016), and Hangzhou Leading Innovation and Entrepreneurship Team Project (No. TD2022007).

Conflict of interest: Y. Hu and L. Feng are employees of ArteryFlow Technology. J. Xiang is the CEO of ArteryFlow Technology. X. Leng is a cofounder of ArteryFlow Technology. The other authors have no conflicts of interest to declare that are relevant to the content of this article.

References

1. Khera AV, Kathiresan S. Genetics of coronary artery disease: discovery, biology and clinical translation. Nat Rev Genet. 2017; 18(6): 331–344, doi: 10.1038/nrg.2016.160, indexed in Pubmed: 28286336.
2. Jia H, Dai J, Hou J, et al. Effective anti-thrombotic therapy without stenting: intravascular optical coherence tomography-based management in plaque erosion (the EROSION study). Eur Heart J. 2017; 38(11): 792–800, doi: 10.1093/eurheartj/ehw381, indexed in Pubmed: 27578806.
3. Windecker S, Kolh P, Alfonso F, et al. 2014 ESC/EACTS Guidelines on myocardial revascularization: The Task Force on Myocardial Revascularization of the European Society of Cardiology (ESC) and the European Association for Cardio-Thoracic Surgery (EACTS)Developed with the special contribution of the European Association of Percutaneous Cardiovascular Interventions (EAPCI). Eur Heart J. 2014; 35(37): 2541–2619, doi: 10.1093/eurheartj/ehu278, indexed in Pubmed: 25173339.
4. Jones DA, Rathod KS, Koganti S, et al. Angiography alone versus angiography plus optical coherence tomography to Guide percutaneous coronary intervention: Outcomes from the Pan-London PCI Cohort. JACC Cardiovasc Interv. 2018; 11(14): 1313–1321, doi: 10.1016/j.jcin.2018.01.274, indexed in Pubmed: 30025725.
5. Huang J, Emori H, Ding D, et al. Diagnostic performance of intracoronary optical coherence tomography-based versus angiography-based fractional flow reserve for the evaluation of coronary lesions. EuroIntervention. 2020; 16(7): 568–576, doi: 10.4244/EIJ-D-19-01034, indexed in Pubmed: 31951207.
6. Lee KE, Lee SHo, Shin ES, et al. A vessel length-based method to compute coronary fractional flow reserve from optical coherence tomography images. Biomed Eng Online. 2017; 16(1): 83, doi: 10.1186/s12938-017-0365-4, indexed in Pubmed: 28651585.
7. Yu W, Huang J, Jia D, et al. Diagnostic accuracy of intracoronary optical coherence tomography-derived fractional flow reserve for assessment of coronary stenosis severity. EuroIntervention. 2019; 15(2): 189–197, doi: 10.4244/EIJ-D-19-00182, indexed in Pubmed: 31147309.
8. Dijkstra EW. A note on two problems in connexion with graphs. Numerische Mathematik. 1959; 1(1): 269–271, doi: 10.1007/bf01386390.
9. van der Zwet PM, Reiber JH. A new approach for the quantification of complex lesion morphology: the gradient field transform; basic principles and validation results. J Am Coll Cardiol. 1994; 24(1): 216–224, doi: 10.1016/0735-1097(94)90566-5, indexed in Pubmed: 8006269.
10. Jiang J, Feng Li, Li C, et al. Fractional flow reserve for coronary stenosis assessment derived from fusion of intravascular ultrasound and X-ray angiography. Quant Imaging Med Surg. 2021; 11(11): 4543–4555, doi: 10.21037/qims-20-1324, indexed in Pubmed: 34737922.
11. Schafer S, Singh V, Hoffmann K, et al. Planning image--guided endovascular interventions: guidewire simulation using shortest path algorithms. SPIE Proceedings. 2007, doi: 10.1117/12.709519.
12. Gibson CM, Cannon CP, Daley WL, et al. TIMI frame count: a quantitative method of assessing coronary artery flow. Circulation. 1996; 93(5): 879–888, doi: 10.1161/01.cir.93.5.879, indexed in Pubmed: 8598078.
13. Tu S, Westra J, Yang J, et al. Diagnostic Accuracy of Fast Computational Approaches to Derive Fractional Flow Reserve From Diagnostic Coronary Angiography: The International Multicenter FAVOR Pilot Study. JACC Cardiovasc Interv. 2016; 9(19): 2024–2035, doi: 10.1016/j.jcin.2016.07.013, indexed in Pubmed: 27712739.
14. Jiang W, Pan Y, Hu Y, et al. Diagnostic accuracy of coronary computed tomography angiography-derived fractional flow reserve. Biomed Eng Online. 2021; 20(1): 77, doi: 10.1186/s12938-021-00914-3, indexed in Pubmed: 34348731.
15. Tonino PAL, De Bruyne B, Pijls NHJ, et al. Fractional flow reserve versus angiography for guiding percutaneous coronary intervention. N Engl J Med. 2009; 360(3): 213–224, doi: 10.1056/NEJMoa0807611, indexed in Pubmed: 19144937.

16. Xaplanteris P, Fournier S, Pijls NHJ, et al. Five-year outcomes with PCI guided by fractional flow reserve. N Engl J Med. 2018; 379(3): 250–259, doi: 10.1056/NEJMoa1803538, indexed in Pubmed: 29785878.
17. Toth GG, Johnson NP, Jeremias A, et al. Standardization of Fractional Flow Reserve Measurements. J Am Coll Cardiol. 2016; 68(7): 742–753, doi: 10.1016/j.jacc.2016.05.067, indexed in Pubmed: 27515335.
18. Toth GG, Toth B, Johnson NP, et al. Revascularization decisions in patients with stable angina and intermediate lesions: results of the international survey on interventional strategy. Circ Cardiovasc Interv. 2014; 7(6): 751–759, doi: 10.1161/CIRCINTERVENTIONS.114.001608, indexed in Pubmed: 25336468.
19. Gutiérrez-Chico JL, Chen Y, Yu W, et al. Diagnostic accuracy and reproducibility of optical flow ratio for functional evaluation of coronary stenosis in a prospective series. Cardiol J. 2020; 27(4): 350–361, doi: 10.5603/CJ.a2020.0071, indexed in Pubmed: 32436590.
20. Di Mario C, Demola P. Morphology and physiology together: Is optical coherence tomography the one-stop-shop of invasive cardiology? Cardiol J. 2020; 27(4): 345–346, doi: 10.5603/CJ.2020.0111, indexed in Pubmed: 32929703.